

Ensemble Feature Extraction for Multi-Container Quality-Diversity Algorithms

Leo Cazenille
Ochanomizu University
Tokyo, Japan
leo.cazenille@gmail.com

ABSTRACT

Quality-Diversity algorithms search for large collections of diverse and high-performing solutions, rather than just for a single solution like typical optimisation methods. They are specially adapted for multi-modal problems that can be solved in many different ways, such as complex reinforcement learning or robotics tasks. However, these approaches are highly dependent on the choice of feature descriptors (FDs) quantifying the similarity in behaviour of the solutions. While FDs usually needs to be hand-designed, recent studies have proposed ways to define them automatically by using feature extraction techniques, such as PCA or Auto-Encoders, to learn a representation of the problem from previously explored solutions. Here, we extend these approaches to more complex problems which cannot be efficiently explored by relying only on a single representation but require instead a set of diverse and complementary representations. We describe MC-AURORA, a Quality-Diversity approach that optimises simultaneously several collections of solutions, each with a different set of FDs, which are, in turn, defined automatically by an ensemble of modular auto-encoders. We show that this approach produces solutions that are more diverse than those produced by single-representation approaches.

CCS CONCEPTS

• Computing methodologies → Search methodologies;

KEYWORDS

Quality-Diversity algorithms, AURORA, Evolutionary Robotics, Ensemble representation learning, Auto-encoders, Deep Learning

1 INTRODUCTION

Designing deep neural network controllers for robotic tasks is still viewed as a complex problem, involving ill-defined objectives and dynamics, unknown and possibly hostile environments, and large experimental variability. One particular challenge is handling complex and uncertain situations that the robot would only be able to overcome by exhibiting behaviours it was not prepared and programmed for. For complex problems, these solutions may be heavily context-dependent, suggesting the use of approaches where the robot would select and adapt its behaviour depending on its environment. These approaches differ from typical search-based and learning-based methods, which usually aim to find one high-performing solution rather than collecting a large number of diverse controllers catering to various environmental contexts.

This paradigm is realised by a recent family of optimisation algorithms named Quality-Diversity (QD) algorithms or Illumination algorithms [10, 14, 14, 40], such as Map-Elites [34] and Novelty Search

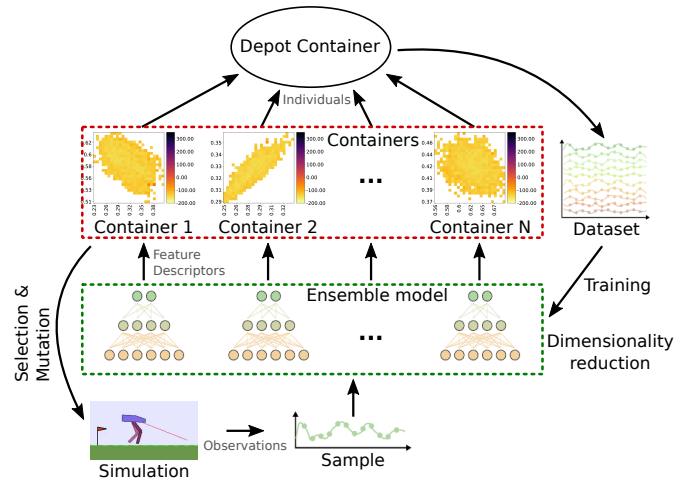


Figure 1: Workflow of MC-AURORA: a Quality-Diversity algorithm explores the behavioural space of a given problem and stores the elite solutions into several containers, each with a different set of feature descriptors (FDs). These FDs are automatically discovered through an ensemble dimensionality reduction technique (e.g. auto-encoders), that is periodically trained on the previously encountered solutions. The multi-container aspect of this method extends the AURORA [11] algorithm to discover automatically an arbitrarily large number of diverse representations of the problem.

with Local Competition [30]. Algorithms like Map-Elites [34] are grid-based, and regroup the explored solutions in a grid (or container [14]) of elites. This produces sets of high-performing solutions that vary according to Feature Descriptors (FDs) represented as axes of the grid. These Feature Descriptors (also called Behavioural Descriptors if they are related to robot behaviours) define a (behavioural) characterisation of the problem and quantify how diverse each controller is from one another.

These algorithms were previously used to solve problems either by efficiently exploring deceptive search spaces [31], or by identifying and exploiting the generated repertoire of solutions [34]. In particular, they are particularly successful in the Evolutionary robotics [13, 17, 33] community, but they were also previously used in Reinforcement Learning [6, 18, 22], for video games [1, 20], in Biology and Chemistry [8, 9, 44], and in problems typically solved with traditional optimisation algorithms [5].

However, in most cases, the human expert must provide the set of FDs used by the QD algorithm to discriminate the different types

of solutions. This choice of FDs may require prior knowledge of the task or a high level of expertise. It will also heavily impact the efficiency of the search process, and results in collections of solutions that are catering to one specific range of interest.

This problem was addressed through several recent studies that defined ways to automatically identify a set of FDs of a problem, without relying on *a-priori* information. Notably, Cully proposed the AURORA ("AUtonomous RObots that Realize their Abilities") algorithm [11] that combined QD with dimensionality reduction (DR) algorithms to perform feature extraction and discover automatically representations of the problem, which were then used as FDs. Indeed, DR methods, such as PCA [37] and Deep auto-encoders [3, 29] are classical tools in Machine Learning and representation learning to extract meaningful low-dimensional representations from high-dimensional data. Usually, a large number of samples are required to train these methods. However, this is not a problem for the AURORA algorithm, as QD algorithms typically explore a large number of solutions which can be, in turn, used to train the DR.

Prior to AURORA, the DeLeNoX was introduced by Liapis *et al.* [32]. It involves two alternating phases: 1) one dimensionality reduction phase computing a diversity measure through a denoising auto-encoder; 2) a novelty-search phase based on this diversity measure. It can thus be seen as a diversity-only version of the AURORA algorithm, without consideration to solution quality.

AURORA also inspired other methods, like the TAXONS [35] algorithm, that searches all potential outcomes of a given problem; or the DDE-Elites [21] algorithm, that conjointly searches and refines a representation of the problem with the help of a Variational Auto-encoder model, and illuminates this search space with adaptive mutation operators.

However, these methods all rely on a single DR instance of the problem, biasing the search process towards a small subset of interesting solution niches in the problem space. AURORA and subsequent algorithms focused on relatively simple benchmark problems that could be characterised with a very small number of FDs (*e.g.* two dimensions). Yet complex problems can be represented in a large (potentially infinite) number of representations, each capturing different aspects of the problem. This property has spurred the representation learning community to come up with DR techniques that can capture a large diversity of features in a problem, a topic known as "ensemble representation learning", involving a collection of various DR modules.

Here, we extend the AURORA algorithm to be able to scale to more complex problems with an arbitrarily large number of distinct representations to code as FDs. This is achieved by enabling AURORA to work with a collection of complementary QD containers (/grids) rather than a single container. Each of these containers has FDs that are defined by a distinct DR module, and DR modules are trained together in an ensemble model. We name this algorithm "**MC-AURORA**": Multi-Container AURORA (Fig. 1).

We test **MC-AURORA** to explore a typical Deep reinforcement problem: the OpenAI Gym BipedalWalker-v3 environment where a bipedal agent must locomote to the end of a slightly uneven randomly generated terrain. We showcase our approach with an ensemble of modular auto-encoders as a DR technique.

We demonstrate that **MC-AURORA** with several containers can find more diverse collections of solution than the original AURORA

algorithm with only one container, and in a more reliable manner. We investigate how the number of containers used can influence the performance of the algorithm. Finally, We present several loss functions that can be applied to the training of the auto-encoders so that the representations found by DR are as different as possible to one another.

2 METHODS

2.1 AURORA

The AURORA algorithm first evaluates a given amount of randomly initialised solutions to compile a dataset of their respective observations matrices. It is used to train the dimensionality reduction algorithm (DR), such as an Auto-Encoder, to learn of (low-dimensional, *e.g.* 2D) latent representation of the observations (a Feature extraction task). This model will serve as a representation of the FD space for the QD container. As such, it can be used to compute the FD of an arbitrary evaluated solution by projecting the latter's observations into the latent space. AURORA proposes two DR methods of choice: Principal Component Analysis (PCA) [37] and Deep (Convolutional) Auto-encoders [3, 29].

Then, AURORA behaves like normal QD algorithm. For each evaluation of the algorithm, 1) a solution is selected in the container, 2) it is varied/mutated, 3) evaluated to compute its fitness and FD (from the latent space projection), 4) and finally an attempt is made to place it into the container. The solutions stored into the container iteratively increase, which also increase the number of observations available to compile the training dataset. This method can work with any kind of containers [14], such as Grid, or Novelty Archives. For instance, the original AURORA paper used Novelty Archive containers with exclusive ϵ -dominance and a self-adaptive novelty threshold parameter.

There are then two strategies for training. With the **Pre-training** strategy, the DR model is never re-trained again after the initial training. With the **Online** strategy, the DR algorithm is periodically re-trained over this dataset (*e.g.* every k iterations, or with a period that decreases exponentially, or even every time k new observations vectors are added). After it is done, the FD of all solutions of the container must be recomputed to use the newly re-trained DR model: this can be done by emptying first the container of all solutions, then recomputing the FD, and finally adding back the solutions one at a time. This may translate into large changes inside the container, as some solutions with previously distinct FD may in turn have very similar FDs after the FD recomputation. In this case, only the best ones are kept, in accordance with the competition mechanism of the QD algorithm.

2.2 Multi-Container AURORA

The original AURORA relies on only one DR model to project observations into their latent representations. As such, it may heavily bias its search process to favour the niches in the FD space that are captured through its DR model, while ignoring others. While this may not be a problem for simpler FD space, it poses the problem of scalability for more complex problems. Moreover, only relying on one model will increase the variability of its accuracy to represent a particular problem depending on its initial conditions (*e.g.* initial weights for a neural network).

Here, we describe a variant of the AURORA algorithm for Multi-container settings. A Multi-container method for Quality-Diversity algorithms ("MCQD") was originally presented in Doncieux *et al.* [16], where a collection of containers of different types could be used concurrently during a single search process. This design is reminiscent of the Island models in Evolutionary Computation, where several populations of solutions are optimised concurrently [43].

In this paper, we show that MCQD and AURORA can be combined to use concurrently a collection of containers, each with a distinct (low-dimensional, *e.g.* 2D) FD space that represents complementary behavioural characterisations and matches different niches in the problem space. This is made possible by using a collection of DR models to represent the FD space of each container.

The workflow of the **MC-AURORA** algorithm is presented in Fig. 1. It is similar to the AURORA algorithm, with a few key differences. First, all containers are initialised with the same collection of randomly initialised solutions. This may translate into redundancies of solutions across containers where a solution can be stored in several containers at the same time, especially if the FD spaces of each container are similar to one another. Second, during the search process, if one solution is added to one of the controllers, it is also stored inside a "depot container", that contain solutions found for all containers. This "depot container" will then serve to compile the training dataset used to train the collection of DR models.

To modulate the number of redundancies across all containers, we consider two strategies. In the **Shared solutions** strategy, each time a new solution is selected, mutated, and evaluated, an attempt is made to add it to every container. With this strategy, good solutions will tend to propagate to all container, reducing the overall diversity of solutions but providing a potential competitive advantage in term of performance. In the **Non-shared solutions** strategy, the search process only focuses on one container at a time: each time a new solution is selected, mutated, and evaluated, an attempt is made to add it to the focused container. Then the focus changes to a different container, with each container having the same budget of evaluations.

For reasons of simplicity, we will use Grid containers instead of the Novelty Archives used in the original AURORA paper. However, our approach could be used with any kind of container.

2.3 Ensemble training of Modular Auto-Encoders

In the field of representation learning, methods exist to train an **ensemble** model composed of several independent modules that are trained on the same dataset [2]. Ensemble models usually combine the outputs of a collection of (potentially diverse) models to obtain enriched output space while controlling variance [24]. Similarly, Reeve *et al.* [41, 42] presented a modular method to train concurrently a diverse ensemble of independent auto-encoders. It allows extracting several distinct sub-sets of features resulting in an enriched latent space representation, with a trade-off between accuracy (reconstruction) and diversity. This method involves the use of a loss function with a diversity component (to ensure that each module is different), which will be presented in the following section.

We consider the following notation: an auto-encoder is composed of two modules: an encoder $E : \mathcal{X} \rightarrow \mathcal{Z}$ and a decoder $D : \mathcal{Z} \rightarrow \mathcal{X}$. Let $\mathcal{X} = \mathbb{R}^{n \times t}$ be the observation space, with n the number of observations per time steps of simulation and t the number of time steps. We set $\mathcal{Z} = \mathbb{R}^d$ as the latent space of the auto-encoder. Let $y = D \circ E(x)$ the output of the auto-encoder for $x \in \mathcal{X}$.

For a training batch \mathbf{x} of size B , we denote $x^{(i)}$ the i th data sample and $z^{(i)} = E(x^{(i)})$ its code. We use the mean squared error (MSE) as the reconstruction loss function:

$$\mathcal{L}_{recons}(X) = \frac{1}{B} \sum_{i=1}^B \left\| D \circ E(x^{(i)}) - x^{(i)} \right\|_2^2$$

As defined in [41], a modular auto-encoder is an ensemble model $\mathcal{W} = \{(E_i, D_i)\}_{i=1}^M$ regrouping M auto-encoder modules (E_i, D_i) . The same paper defines a loss function designed to increase the diversity of the auto-encoder modules, and based on the reconstructed outputs of each module. It is defined as:

$$\mathcal{L}_{outputs}(\mathcal{W}, X) = \frac{1}{B} \frac{1}{M} \sum_{i=1}^B \sum_{j=1}^M \left\| D_j \circ E_j(x^{(i)}) - \frac{1}{M} \sum_{k=1}^M D_j \circ E_j(x^{(k)}) \right\|_2^2 \quad (1)$$

This loss function is combined with the reconstruction loss as follows:

$$\mathcal{L}(\mathcal{W}, X) = \mathcal{L}_{recons}(\mathcal{W}, X) - \lambda \mathcal{L}_{outputs}(\mathcal{W}, X) \quad (2)$$

where λ is a weighting parameter to define the importance of diversity compared to reconstruction.

In this paper, we also consider alternative loss functions to enforce diversity in modular Auto-Encoder. We postulate that diversity in latent representations can be obtained through loss functions based on the latent representation rather than reconstructed outputs. We want to constrain the latent representation of each container to behave as differently as possible from one another. This can be achieved through covariance-based statistics of either all the regrouped latent spaces of all containers or by comparing each latent space with one another. As such we define two loss functions as follows:

We define the following loss function computed using the mean magnitude of the covariance matrix (inspired from [28]):

$$\mathcal{L}_{cov}(\mathcal{W}, X) = \sum_{i=1}^d \sum_{j=1, i \neq j}^d |cov(X)_{i,j}| \quad (3)$$

where $cov(X)_{i,j}$ is the i, j element of the covariance matrix of X . This loss function can be used in Eq. 2 instead of $\mathcal{L}_{outputs}(\mathcal{W}, X)$

We take inspiration the Correlation Matrix Distance defined in [25], and define the following loss function: We set R_1, \dots, R_m the correlation matrices between each elements of the respective auto-encoders modules $\{(E_i, D_i)\}$.

$$d_{corr}(H_1, H_2) = 1 - \frac{tr\{H_1 H_2\}}{\|H_1\|_f \|H_2\|_f} \in [0, 1] \quad (4)$$

where $\|\cdot\|_f$ is the Frobenius norm, and $tr\{\cdot\}$ the matrix trace.

$$\mathcal{L}_{cmd}(\mathcal{W}, X) = \sum_{i=1}^d \sum_{j=1, i \neq j}^d d_{corr}(R_i, R_j) \quad (5)$$

2.4 Post-processing

Artificial Neural Network models trained through a gradient-based approach tend to favour data following normal distributions. This is also the case for the latent representations of auto-encoders. However, most Quality-Diversity algorithms use containers (including Grids and Novelty Archives) that are designed for FD following a uniform distribution (*i.e.* uniform bins for Grids, constant novelty thresholds for Archives). As such, containers using the latent representation to define their FD space may have an artificially lowered coverage: Grids will have a lot of emptied bins and Archives will be artificially more sparse. Moreover, the FD space will be denser the closer to the distribution mean, resulting in non-uniform levels of competition between elites over the entire container.

Here, we propose to alleviate these problems by transforming the latent distributions to a uniform distribution ($\in [0, 1]$) by using Quantile Transformations [38], a methodology commonly used in Machine Learning to normalise data-sets.

The **MC-AURORA** algorithm was coded using the Python Quality-Diversity library QDpy [7] version 0.1.2.1. All deep neural networks models are implemented with the PyTorch [36] library version 1.7.1. All source codes are available at: <https://github.com/leo-cazenille/multiAE-ME>.

3 EXPERIMENTAL VALIDATION

All experimental cases considered are listed in Table 1, and described in the following subsections. All tested algorithms are repeated 20 times and use the hyper-parameters listed in Table 2. All containers of all cases are initialised with a collection of 10000 solutions (with genomes following a random uniform distribution). This same collection is also used as the initial training data-set for the auto-encoders.

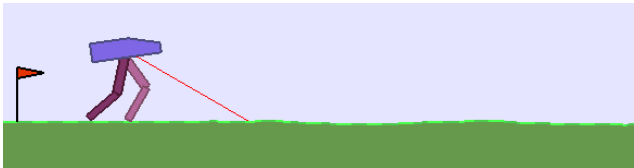


Figure 2: Example frame of the OpenAI Gym [4] BipedalWalker-v3 environment where a robot with two legs and equipped with a lidar aims to move forward as far as possible in a stochastic environment.

3.1 The BipedalWalker-v3 environment

We test the performance of the **MC-AURORA** algorithm over the OpenAI Gym [4] BipedalWalker-v3 environment, a classical benchmark in the Reinforcement Learning and Quality-Diversity literature (Fig. 2). This benchmark is more complex than those originally presented in the AURORA paper [11], with behaviours that can be characterised in numerous complementary ways, making it relevant as a benchmark for this study.

The BipedalWalker-v3¹ environment consists of a two-legged walking simulated agent that must locomote to the end of a slightly

¹https://github.com/openai/gym/blob/master/gym/envs/box2d/bipedal_walker.py

uneven randomly generated terrain in a limited amount of time. The agent is equipped with four torque-controlled motor driven joints. The 24 parameter state space includes position, hull angle, jumping, hip and knee joint angles/velocities, and a ten-point lidar range finder. The continuous action space is the four motor controlled torque values. The objective of the agent is to locomote the agent to the end of the environment. A positive reward is awarded for moving towards the goal, with an added bonus related to the stability of the hull. Motor efficiency is awarded a negative reward for the use of torque while a negative reward of -100 is awarded when the agent falls.

Note that, we use a **simplified version** of the BipedalWalker-v3 benchmark with **only 300 steps per episode, instead of the default 3000**. Observations are also averaged over 30 time-steps (so there are 10 averaged state values per evaluation), and each evaluation is computed over 5 episodes. Each evaluation has thus $10 * 24 * 5 = 1200$ observations, which is lower than for the standard version (180000 observations per evaluation), making it simpler to model with an auto-encoder. The best fitness found are also around nine times lower (40) than the maximum obtainable of 350. The agent is controlled with an MLP controlled with a topology from the literature², as defined in Table 2.

Benchmarking Quality-Diversity algorithms with a BipedalWalker environment was pioneered by the work of Justensen *et al.* [26] where an adaptive sampling methodology was used to handle the stochasticity of this benchmark. Here, we use a simpler scheme to handle stochasticity, with fitness and FD averaged explicitly over the results of five episodes. The subsequent work of Gupta *et al.* [22] used this approach to compare the performance of MAP-Elites and policy gradients algorithms trained with intrinsic curiosity loss. This last work also presented the following set of human-designed FD (averaged over one episode) used to characterise the behaviour of the agent: *Distance* is the agent’s position relative to the goal, *Hull angle* is the angle of the body of the agent, *Torque* is the force applied to the agent’s hip and knee joints, *Jump* describes when both legs simultaneously are contact-less with the environment, *Hip and knee angles* describe the agent’s leg joint angles, *Hip and knee speeds* describes the agent’s leg joint angle speeds.

As a reference experimental case, we test the performance of MAP-Elites over this benchmark with a similar set of hand-designed FDs as [22], with the exclusion of **Hip and knee speeds** (for the sake of simplicity). We consider three experimental cases with these FDs. First, **hardcoded-4** involves four bi-dimensional grids with shared solutions and with the following FDs pairs: (1) Distance vs. Hull Angle (directly correlated to the extrinsic reward); (2): Torque vs. Jump (impacts the overall efficiency of the agent); (3) and (4): joint angles between hips and knees for respectively the first and second legs. Second, **hardcoded-4-ns** is a similar case, but with non-shared solutions. Lastly, **hardcoded-1** only has one grid with the (1) pair of FD.

3.2 Metrics

Studied experimental cases are quantitatively compared through the following set of metrics. First, we assess the general performance and diversity of the solutions found at the last iteration of the

²<http://blog.otoro.net/2017/11/12/evolving-stable-strategies/>

	Case Name	FD type	Shared solutions	Training type	Loss	Nr. of grids	Grids shape
Base	hardcoded-4	Hardcoded	Yes	None	None	4	25x25
	hardcoded-4-ns	Hardcoded	No	None	None	4	25x25
	pt-reco-4	AE	Yes	Pre-trained	Reconstruction	4	25x25
	reco-4	AE	Yes	Online	Reconstruction	4	25x25
	qt-reco-4	AE+QT	Yes	Online	Reconstruction	4	25x25
	qt-reco-4-ns	AE+QT	No	Online	Reconstruction	4	25x25
Nr. of Grids	hardcoded-1	Hardcoded	-	None	None	1	50x50
	qt-reco-1	AE+QT	-	Online	Reconstruction	1	50x50
	qt-reco-6-ns	AE+QT	No	Online	Reconstruction	6	5*20x20 + 1*20x25
	qt-reco-9-ns	AE+QT	No	Online	Reconstruction	9	8*17x16 + 1*18x18
	qt-reco-25-ns	AE+QT	No	Online	Reconstruction	25	10x10
	Loss	qt-outputs-4-ns	AE+QT	No	Online	Reconstruction+1*Outputs	4
qt-covmin-4-ns		AE+QT	No	Online	Reconstruction+1*COV	4	25x25
qt-covmax-4-ns		AE+QT	No	Online	Reconstruction-1*COV	4	25x25
qt-cmd-4-ns		AE+QT	No	Online	Reconstruction+1*CMD	4	25x25

Table 1: List of all experimental cases. All cases have the same budget of 2500 bins over all their containers.

	Parameter Name	Value
Simulation	Episodes per eval.	5
	Max episode length	300 (instead of the default 3000)
	Controller topology	MLP 2 hidden layers 40x40, tanh activation
	Prob. dimensionality	2804
Illumination	Grid total nr. of bins	2500
	Evaluation budget	100000 (excl. initialisation)
	Initialisation budget	10000 (random uniform)
	Batch size	1000 Evaluations
	Selection	Curiosity roulette (Score-proportionate) [14]
	Mutation	Polynomial bounded [15, 34]
	Mutation probability	0.1
	ETA [15]	20 (Mutation Crowding degree)
Feature-extraction	Encoder topology	Two Conv1d (kernel size=3) with batchnorm and ELU activation, two dense of 5 then 2 neurons with dropouts (0.2) and Sigmoid activation
	Decoder topology	Two dense of 2 then 5 neurons with dropouts (0.2) and ELU activation, two ConvTranspose1d (kernel size=3) with MaxUnpool1d, batchnorm and ELU activation, one dense with Sigmoid activation
	Weight initialization	Xavier uniform
	Training period	5000 solutions added to the depot container
	Optimiser	Adam
	Nr. of epochs	200
	Learning rate	0.1
	Batch size	1024
	Validation split	0.25
	Diversity coeff.	1.0

Table 2: Hyper-parameters used for all experiments.

algorithms, through the coverage (nr. of occupied bins), QD-score (sum of fitness normalised to $[0, 1]$ of all solutions in the containers), and best-fitness metrics.

Good solutions tend to propagate through several containers at the same time (including the initial 10000 solutions), especially in shared solutions cases. It may lead to a degree of solution redundancy across several containers. As such, two versions of the

previously-defined metrics are considered: the **base** version is computed over all solutions found in all containers; the **unique** version takes into account the redundancy of solutions across several containers, and only count redundant solutions once. We also assess the proportion of redundant solutions through a Container Redundancy metric, defined as: $1 - R/S$ with R the number of redundant solutions and $S = 2500$ the sum of the capacity (*i.e.* the number of bins) of each container.

We postulate that this redundancy, and also the general performance and diversity is highly dependant on the correlation between the FD used for all containers. As such, we define a metric termed "FD absolute correlation" computed as the mean magnitude (absolute value) of the correlation matrix components of the FD or all containers. A high score of this metric would translate into FD space that characterise highly similar behaviours across all containers.

3.3 Results

Experimental cases are compared using the previously defined metrics across 20 runs. We consider all cases listed in Table 1. Table 3 regroups most of these statistics at the last iteration of all cases.

3.3.1 Training and Shared solution strategies. We will first compare the performances of the "Base" cases listed in Table 1.

Figure 3 shows representative examples of the four grids found by the **hardcoded-4**, **reco-4** and **qt-reco-4** cases. The last two grids of the **hardcoded-4** looks symmetrical, suggesting that their FD (joint angles between hips and knees) are heavily correlated. The **reco-4** FD spaces all follow normal distributions, with a large number of inaccessible bins. The **qt-reco-4** occupy nearly all possible bins.

The statistics in Table 3 indicate that the human-designed FD are heavily correlated both in the **hardcoded-4** and **hardcoded-4-ns** cases. This translates into container redundancy above 35%. The large difference in both coverage and QD-score between **hardcoded-4** and **hardcoded-4-ns** suggests than the "Non-sharing" strategy can negatively affect both performance and diversity when the FD can heavily correlated.

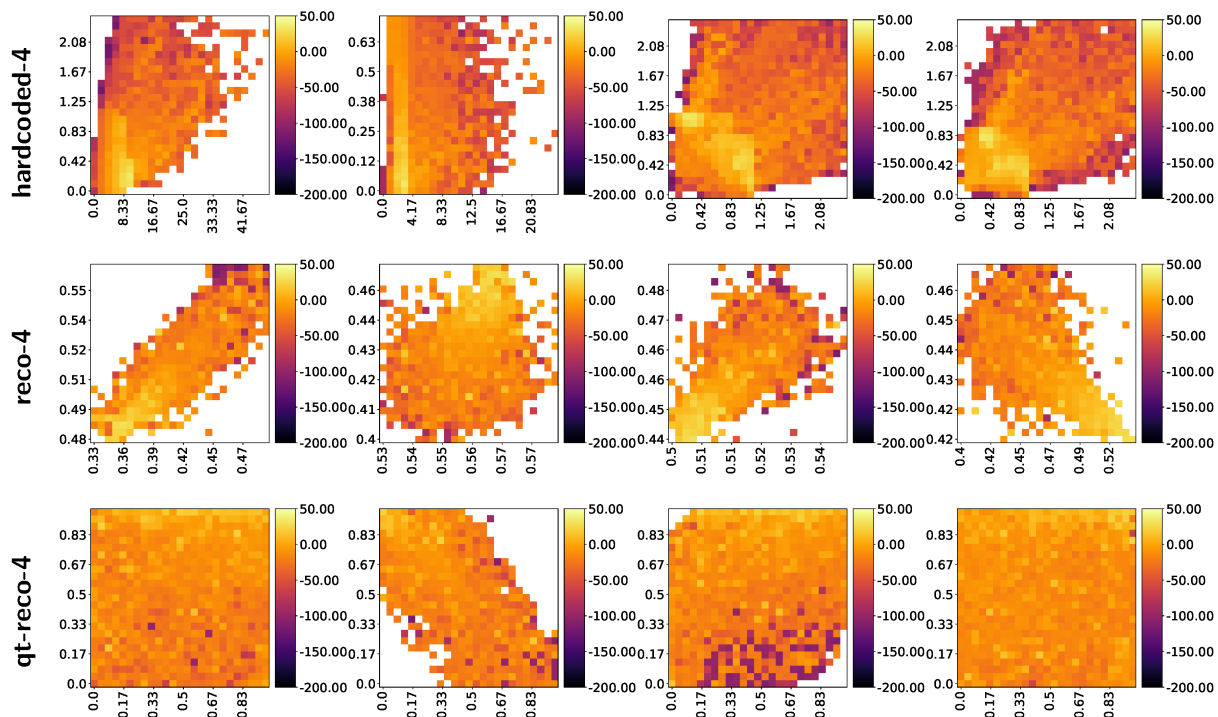


Figure 3: Instances of the four grids of solutions found by three representative cases: `hardcoded-4` where the FD are hand-crafted by the expert, `reco-4` where the FD are the latent space of an Auto-Encoder, `qt-reco-4` where we post-process this latent space with a quantile transformation [38] to follow a $[0, 1]$ uniform distribution. All cases have the same budget of 2500 grid bins.

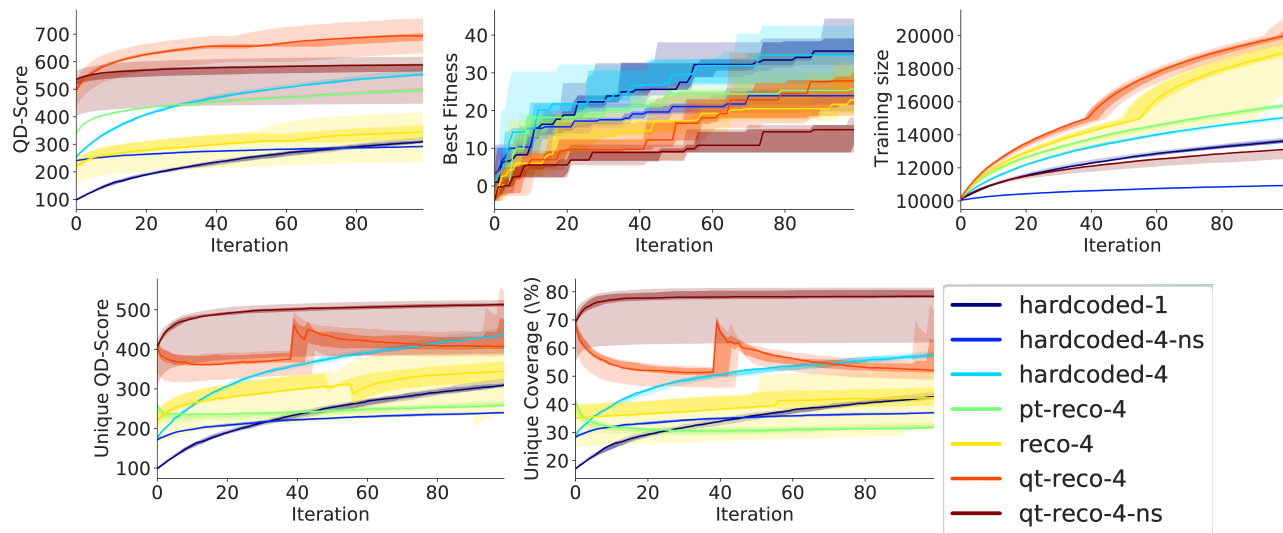


Figure 4: Comparison of seven representative cases across the following metrics: (top) the QD-Score and best-ever fitness of solutions stored in all containers; (top right) depot container (auto-encoders training dataset) size; (bottom) the QD-Score and coverage of all unique solution stored in all containers (*i.e.* without taking in account redundant solutions). Solid lines represent the mean of values across 20 runs. Light and dark shades correspond respectively to min-max values and 25th-75th quantiles.

	Unique QD-Score	Unique Coverage (%)	QD-Score	Coverage (%)	Best Fitness	FD Abs. Corr.	Cont. Redundancy
hardcoded-4	439.360 ± 7.471	57.680 ± 0.900	557.496 ± 8.885	72.208 ± 1.142	33.229 ± 5.781	0.575 ± 0.009	0.368 ± 0.006
hardcoded-4-ns	239.614 ± 2.857	36.968 ± 0.398	291.560 ± 2.817	45.160 ± 0.390	25.353 ± 4.828	0.660 ± 0.009	0.352 ± 0.001
pt-reco-4	261.242 ± 5.893	32.240 ± 0.833	497.007 ± 4.894	59.320 ± 0.770	26.905 ± 2.866	0.277 ± 0.045	0.723 ± 0.014
reco-4	314.882 ± 44.915	39.232 ± 5.106	314.882 ± 44.915	39.232 ± 5.106	24.614 ± 4.348	0.483 ± 0.323	0.684 ± 0.006
qt-reco-4	473.456 ± 67.374	60.552 ± 8.324	722.727 ± 68.967	90.152 ± 7.558	23.319 ± 5.246	0.328 ± 0.071	0.553 ± 0.090
qt-reco-4-ns	505.298 ± 46.870	77.248 ± 5.879	574.096 ± 57.843	88.112 ± 7.065	17.078 ± 3.104	0.302 ± 0.058	0.241 ± 0.027
hardcoded-1	320.762 ± 16.747	43.832 ± 2.551	320.762 ± 16.747	43.832 ± 2.551	34.255 ± 5.490	0.581 ± 0.029	0.000 ± 0.000
qt-reco-1	602.999 ± 93.807	94.856 ± 8.113	602.999 ± 93.807	94.856 ± 8.113	14.067 ± 4.103	0.072 ± 0.127	0.000 ± 0.000
qt-reco-6-ns	590.995 ± 35.041	83.568 ± 4.252	631.452 ± 44.386	89.512 ± 5.276	19.206 ± 6.155	0.268 ± 0.019	0.130 ± 0.013
qt-reco-9-ns	604.357 ± 30.788	78.176 ± 3.370	606.429 ± 37.204	89.976 ± 3.692	23.998 ± 4.371	0.282 ± 0.027	0.217 ± 0.045
qt-reco-25-ns	446.305 ± 9.096	63.872 ± 1.240	653.876 ± 10.931	92.440 ± 1.139	20.672 ± 4.173	0.267 ± 0.017	0.468 ± 0.010
qt-outputs-4-ns	538.816 ± 24.450	80.120 ± 4.047	598.385 ± 32.554	90.728 ± 5.398	19.733 ± 3.155	0.262 ± 0.012	0.225 ± 0.019
qt-covmin-4-ns	507.327 ± 42.212	77.280 ± 5.658	572.712 ± 53.720	87.368 ± 7.125	16.968 ± 5.626	0.287 ± 0.054	0.293 ± 0.022
qt-covmax-4-ns	528.666 ± 30.037	79.056 ± 5.066	571.542 ± 32.726	87.352 ± 5.813	17.850 ± 3.750	0.244 ± 0.048	0.192 ± 0.024
qt-cmd-4-ns	539.779 ± 22.647	79.784 ± 2.878	597.727 ± 33.805	90.096 ± 4.073	19.144 ± 3.546	0.252 ± 0.034	0.224 ± 0.019

Table 3: Mean statistics of all studied cases at the last iteration (100th) over 20 runs. The numbers following the symbol ± represent the standard deviation. The QD-Score and coverage metrics take into account redundancies, while their "unique" versions only take into account redundant solutions once.

The online case **reco-4** is superior to the pre-trained case **pt-reco-4** in most beneficial statistics: it has a higher Unique QD-Score and Unique Coverage, less redundancy, and less FD correlations. Similarly, cases with Quantile transform post-processing are superior to cases without post-processing.

Both the **qt-reco-4** and **qt-reco-4-ns** cases outperform the cases with human-designed FD, possibly because the Quantile transform maximise the number of bins that are occupied. However, this translates into less pressure toward competition, explaining why the best-performing individuals have a lower fitness than the best-performing solutions found by the **hardcoded-4** and **hardcoded-4-ns** case. Having a higher redundancy (which would suggest more competition between solutions) does not necessarily translate into higher best fitness scores, as shown by case **pt-reco-4**.

The **qt-reco-4-ns** is the "Base" case with the highest Unique QD-Score and Unique coverage, but the lowest best-fitness. We postulate that this is still related to solution competition because of the higher number of unique bins, and it might be alleviated by increasing the total budget of evaluations.

All the online cases display a far larger variability in term of (Unique) QD-score, coverage and FD correlation than the human-designed FD cases and pre-trained cases, suggesting that solution diversity is heavily affected by the resulting auto-encoder models.

All these results are corroborated in Fig. 4 which shows a comparison of the "Base" cases across a number of metrics and with respect to iterations. Note that the Unique QD-Score and Unique Coverage metrics show that several cases, especially cases with a "Shared solutions" strategy, may have a spike in value just after re-training. However, this spike may quickly degrade as good solutions propagate into several containers, increasing redundancy. This is one advantage of cases with a "Non-shared solutions" strategy, that do not have any easily perceived spike after re-training.

3.3.2 Impact of number of containers. We will now compare cases with differing number of containers, as listed in the "Nr. of Grids" section of Table 1.

The **hardcoded-1** case has lower QD-Score and coverage scores compared to **hardcoded-4**, possibly because its FD pair translates into the sparsest grid, as seen in Fig. 3. However, this results in more competition, which explains its high best-fitness score.

The **qt-reco-1** case only has one container, and such, does not have any redundancy. This explains why it has a higher Unique QD-score than **qt-reco-4-ns**, even through its QD-Score is lower than the latter. It is also the case with the higher variability of (Unique) QD-Score suggesting that, on setting with only one container, solution diversity is heavily dependent on the kind of representation learning by the auto-encoder.

In most scores, **qt-reco-9-ns** outperforms **qt-reco-6-ns** which outperforms **qt-reco-4-ns** which outperforms **qt-reco-25-ns**, suggesting that the increasing the number of container is beneficial, up to a point (here around 9 containers, and lower than 25). It is also especially relevant to decrease the variability in (Unique) QD-Score and coverage, with **qt-reco-25-ns** having the lowest variability over these statistics.

3.3.3 impact of AE loss. Here, we compare cases modular auto-encoder models training with a loss function with a diversity component. All cases training in such a manner outperform the **qt-reco-4-ns** case in most scores, except with the Best-fitness scores which are mostly the same. The best scores are obtained by the **qt-cmd-4-ns** and **qt-outputs-4-ns** cases, with similar Unique QD-Scores, Unique coverage scores and redundancy.

The case **qt-covmin-4-ns**, designed to increase the covariance between FD, displays a higher FD correlation than **qt-covmax-4-ns**. Surprisingly, it also shows a lower FD correlation score than **qt-reco-4-ns**, possibly due to the diversity component of the loss function helping the gradient-descent process.

4 DISCUSSION AND CONCLUSIONS

In this paper, we presented **MC-AURORA**, a variant of the **AURORA** algorithm able to automatically find several distinct and complementary behavioural characterisations of the solutions of a problem in an unsupervised manner. While **AURORA** provided

this capability to single-container setups with relatively low dimensional FD spaces, we extended this approach to scale to more complex problems that could be represented in a large number of ways, potentially translating into prohibitively large FD spaces.

Our approach relies on ensemble dimensionality reduction techniques, such as Deep Convolutional Auto-Encoders, that are trained on previously encountered solutions to identify the FD of all containers. QD algorithms usually assume a uniform distribution over the FD space. However, Auto-Encoders latent representations follows normal distributions, resulting in a non-linear amount of solution competition depending on their position in the FD space. We describe a post-processing method to alleviate this problem.

We investigated the interplay between containers: notably, we described how to avoid or make use of solution redundancy over all containers, and how the number of containers could affect performance and diversity. Our results show that tuning the number of containers can have huge impact on the performance and diversity of the solution. Having larger numbers of containers also reduces Unique QD-Score and Coverage variability.

We showed that it is possible to affect the performance and diversity of solutions found with **MC-AURORA** by training the auto-encoders with a loss function including a diversity component. We tested three types of diversity loss: either based on the reconstructed outputs, or related to the covariance and correlation between FD. Our results suggest than having both a reconstruction and diversity component in the loss function is mostly beneficial compared to just having a reconstruction. However, this is less beneficial than correctly tuning the number of containers, with **qt-reco-9-ns** having the best overall results in all cases.

Our approach could be improved further in several ways. First, we could use different auto-encoder topologies to cope with highly dimensional observations (e.g. LSTM or Transformers). Here, we only used an homogeneous topology for all containers, but several topologies could be used concurrently, to further increase diversity.

Second, we only accounted for simulation stochasticity through a simple explicit averaging scheme. However, recent studies described more complex methods to handle noise with Quality-Diversity algorithms, possibly through adaptive [26] or implicitly averaging [19], or by using a Variational Auto-encoder [21].

Third, it would be interesting to investigate fine-grained control of solution redundancy across containers, to reduce or dynamically tune their number. In a future paper, we will describe how another post-processing operation commonly used in Machine Learning known as "whitening" [23, 27] could be used to further decorrelate the FD space and reduce the number of redundancies.

Finally, it may be possible to automatically and dynamically adapt the evaluation budget of the collection of containers by using a multi-container version of ME-MAP-Elites [12] to dynamically give more evaluation budget to containers depending on their statistics such as coverage, QD-score, redundancy, best-ever, etc. This topic will be addressed in a future paper.

ACKNOWLEDGMENTS

This work was supported by Grant-in-Aid for JSPS Fellows JP19F19722.

REFERENCES

- [1] A Alvarez, S Dahlskog, J Font, and J Togelius. 2019. Empowering Quality Diversity in Dungeon Design with Interactive Constrained MAP-Elites. *arXiv preprint arXiv:1906.05175* (2019).
- [2] V Bolón-Canedo and A Alonso-Betanzos. 2019. Ensembles for feature selection: A review and future trends. *Information Fusion* 52 (2019), 1–12.
- [3] H Boulard and Y Kamp. 1988. Auto-association by multilayer perceptrons and singular value decomposition. *Biological cybernetics* 59, 4 (1988), 291–294.
- [4] G Brockman, V Cheung, L Pettersson, J Schneider, J Schulman, J Tang, and W Zaremba. 2016. Openai gym. *arXiv preprint arXiv:1606.01540* (2016).
- [5] JP Bruneton, L Cazenille, A Douin, and V Reverdy. 2019. Exploration and Exploitation in Symbolic Regression using Quality-Diversity and Evolutionary Strategies Algorithms. *arXiv preprint arXiv:1906.03959* (2019).
- [6] S Brych and A Cully. 2020. Competitiveness of MAP-Elites against Proximal Policy Optimization on locomotion tasks in deterministic simulations. *arXiv preprint arXiv:2009.08438* (2020).
- [7] L Cazenille. 2018. QDPY: A Python framework for Quality-Diversity. <https://gitlab.com/leo.cazenille/qdpy>.
- [8] L Cazenille, N Bredeche, and N Aubert-Kato. 2019. Exploring self-assembling behaviors in a swarm of bio-micro-robots using surrogate-assisted map-elites. In *2019 IEEE Symposium Series on Computational Intelligence (SSCI)*. IEEE, 238–246.
- [9] L Cazenille, N Bredeche, and J Halloy. 2019. Automatic Calibration of Artificial Neural Networks for Zebrafish Collective Behaviours using a Quality Diversity Algorithm. In *Conference on Biomimetic and Biohybrid Systems*. Springer, 38–50.
- [10] K Chatzilygeroudis, A Cully, V Vassiliades, and JB Mouret. 2020. Quality-Diversity Optimization: a novel branch of stochastic optimization. *arXiv preprint arXiv:2012.04322* (2020).
- [11] A Cully. 2019. Autonomous skill discovery with quality-diversity and unsupervised descriptors. In *Proceedings of the Genetic and Evolutionary Computation Conference*. 81–89.
- [12] A Cully. 2020. Multi-Emitter MAP-Elites: Improving quality, diversity and convergence speed with heterogeneous sets of emitters. *arXiv preprint arXiv:2007.05352* (2020).
- [13] A Cully, J Clune, D Tarapore, and JB Mouret. 2015. Robots that can adapt like animals. *Nature* 521, 7553 (2015), 503.
- [14] A Cully and Y Demiris. 2018. Quality and diversity optimization: A unifying modular framework. *IEEE Transactions on Evolutionary Computation* 22, 2 (2018), 245–259.
- [15] K Deb, A Pratap, S Agarwal, and T Meyarivan. 2002. A fast and elitist multiobjective genetic algorithm: NSGA-II. *IEEE transactions on evolutionary computation* 6, 2 (2002), 182–197.
- [16] S Doncieux and A Coninx. 2018. Open-ended evolution with multi-containers QD. In *Proceedings of the Genetic and Evolutionary Computation Conference Companion*. 107–108.
- [17] M Duarte, J Gomes, SM Oliveira, and AL Christensen. 2018. Evolution of repertoire-based control for robots with complex locomotor systems. *IEEE Transactions on Evolutionary Computation* 22, 2 (2018), 314–328.
- [18] A Ecoffet, J Huizinga, J Lehman, KO Stanley, and J Clune. 2019. Go-Explore: a New Approach for Hard-Exploration Problems. *arXiv preprint arXiv:1901.10995* (2019).
- [19] M Flageat and A Cully. 2020. Fast and stable MAP-Elites in noisy domains using deep grids. In *Artificial Life Conference Proceedings*. MIT Press, 273–282.
- [20] MC Fontaine, J Togelius, S Nikolaidis, and AK Hoover. 2020. Covariance Matrix Adaptation for the Rapid Illumination of Behavior Space. In *Proceedings of the Genetic and Evolutionary Computation Conference Companion*. ACM.
- [21] A Gaier, A Asteroth, and JB Mouret. 2020. Discovering representations for black-box optimization. In *Proceedings of the 2020 Genetic and Evolutionary Computation Conference*. 103–111.
- [22] V Gupta, N Aubert-Kato, and L Cazenille. 2020. Exploring the BipedalWalker benchmark with MAP-Elites and curiosity-driven A3C. In *Proceedings of the 2020 Genetic and Evolutionary Computation Conference Companion*. 79–80.
- [23] S Hahn and H Choi. 2019. Disentangling Latent Factors of Variational Auto-encoder with Whitening. In *International Conference on Artificial Neural Networks*. Springer, 590–603.
- [24] T Hastie, R Tibshirani, and J Friedman. 2009. *The elements of statistical learning: data mining, inference, and prediction*. Springer Science & Business Media.
- [25] M Herdin, N Czink, H Ozelcik, and E Bonek. 2005. Correlation matrix distance, a meaningful measure for evaluation of non-stationary MIMO channels. In *2005 IEEE 61st Vehicular Technology Conference*, Vol. 1. IEEE, 136–140.
- [26] N Justesen, S Risi, and JB Mouret. 2019. MAP-Elites for noisy domains by adaptive sampling. In *Proceedings of the Genetic and Evolutionary Computation Conference Companion*. ACM, 121–122.
- [27] A Kessy, A Lewin, and K Strimmer. 2018. Optimal whitening and decorrelation. *The American Statistician* 72, 4 (2018), 309–314.
- [28] S Ladjal, A Newson, and C Pham. 2019. A PCA-like autoencoder. *arXiv preprint arXiv:1904.01277* (2019).

- [29] Y Le Cun. 1986. Learning process in an asymmetric threshold network. In *Disordered systems and biological organization*. Springer, 233–240.
- [30] J Lehman and KO Stanley. 2011. Evolving a diversity of virtual creatures through novelty search and local competition. In *Proceedings of the 13th annual conference on Genetic and evolutionary computation*. ACM, 211–218.
- [31] J Lehman, KO Stanley, and R Miikkilainen. 2013. Effective diversity maintenance in deceptive domains. In *Proceedings of the 15th annual conference on Genetic and evolutionary computation*. ACM, 215–222.
- [32] A Liapis, HP Martínez, J Togelius, and GN Yannakakis. 2013. Transforming exploratory creativity with DeLeNoX. In *4th International Conference on Computational Creativity, ICC3 2013*. Faculty of Architecture, Design and Planning, The University of Sydney, 56–63.
- [33] JB Mouret. 2020. Evolving the behavior of machines: from micro to macroevolution. *iScience* (2020), 101731.
- [34] JB Mouret and J Clune. 2015. Illuminating search spaces by mapping elites. *arXiv preprint arXiv:1504.04909* (2015).
- [35] G Paolo, A Laflaquiere, A Coninx, and S Doncieux. 2020. Unsupervised learning and exploration of reachable outcome space. In *2020 IEEE International Conference on Robotics and Automation (ICRA)*. IEEE, 2379–2385.
- [36] A Paszke, S Gross, F Massa, A Lerer, J Bradbury, G Chanan, T Killeen, Z Lin, N Gimelshein, L Antiga, A Desmaison, A Kopf, E Yang, Z DeVito, M Raison, A Tejani, S Chilamkurthy, B Steiner, L Fang, J Bai, and S Chintala. 2019. PyTorch: An Imperative Style, High-Performance Deep Learning Library. In *Advances in Neural Information Processing Systems 32*, H. Wallach, H. Larochelle, A. Beygelzimer, F. d’Alché-Buc, E. Fox, and R. Garnett (Eds.). Curran Associates, Inc., 8024–8035. <http://papers.neurips.cc/paper/9015-pytorch-an-imperative-style-high-performance-deep-learning-library.pdf>
- [37] K Pearson. 1901. LIII. On lines and planes of closest fit to systems of points in space. *The London, Edinburgh, and Dublin Philosophical Magazine and Journal of Science* 2, 11 (1901), 559–572.
- [38] F Pedregosa, G Varoquaux, A Gramfort, V Michel, B Thirion, O Grisel, M Blondel, P Prettenhofer, R Weiss, V Dubourg, J Vanderplas, A Passos, D Cournapeau, M Brucher, M Perrot, and E Duchesnay. 2011. Scikit-learn: Machine Learning in Python. *Journal of Machine Learning Research* 12 (2011), 2825–2830.
- [39] A Péré, S Forestier, O Sigaud, and PY Oudeyer. 2018. Unsupervised learning of goal spaces for intrinsically motivated goal exploration. *arXiv preprint arXiv:1803.00781* (2018).
- [40] JK Pugh, LB Soros, and KO Stanley. 2016. Quality diversity: A new frontier for evolutionary computation. *Frontiers in Robotics and AI* 3 (2016), 40.
- [41] H Reeve and G Brown. 2015. Modular autoencoders for ensemble feature extraction. In *Feature Extraction: Modern Questions and Challenges*. PMLR, 242–259.
- [42] HWJ Reeve and G Brown. 2018. Diversity and degrees of freedom in regression ensembles. *Neurocomputing* 298 (2018), 55–68.
- [43] Z Skolicki. 2005. An analysis of island models in evolutionary computation. In *Proceedings of the 7th annual workshop on Genetic and evolutionary computation*. 386–389.
- [44] J Verhellen and J Van den Abeele. 2020. Illuminating elite patches of chemical space. *Chemical Science* (2020).

A PAIRWISE KL-COVERAGE

We consider another way of comparing together the FD spaces, by using the KL-Coverage metric from [39], which was also used in the original AURORA paper [11], to check whether two FD spaces are similar to each other (possibly hinting at their representation capabilities). We extend the original definition to handle multi-containers scenarios:

$$KLC = \sum_c \mathcal{D}_{KL}[E_c||A_c] = \sum_c \sum_{i=1}^{10} E_c(i) \log\left(\frac{E_c(i)}{A_c(i)}\right) \quad (6)$$

where C is the set of all containers; and for a container c : E_c and A_c are respectively the reference and the compared distributions for container c . Lower KLC scores indicate more similar FD spaces.

Table 4 contains a pairwise comparison of the distribution of all solutions found by each case, by using the KL coverage metric.

The results in Table 4 show that the distributions of solutions of pre-trained and online cases are larger than the ones of the human-designed cases (with low pairwise KL-coverage scores when human-designed cases are used to compute reference distributions). The **pt-reco-4** has a very dissimilar distribution of solutions compared to the other cases, possibly because of its high redundancy.

	hardcoded-4	hardcoded-4-ns	pt-reco-4	qt-reco-4-ns	hardcoded-1	qt-reco-1	qt-reco-9-ns	qt-reco-25-ns	qt-outputs-4-ns	qt-covmin-4-ns	qt-covmax-4-ns	qt-cmd-4-ns
hardcoded-4	3.532 ± 2.279	37.529 ± 5.204	237.401 ± 138.267	67.478 ± 58.851	45.213 ± 9.204	15.145 ± 26.647	110.498 ± 60.944	381.826 ± 103.125	33.672 ± 24.755	41.156 ± 53.640	88.725 ± 90.881	64.773 ± 68.020
hardcoded-4-ns	2.161 ± 0.703	6.556 ± 4.013	217.568 ± 30.985	60.626 ± 55.809	28.818 ± 6.043	13.950 ± 24.685	110.802 ± 51.521	372.828 ± 83.181	29.310 ± 24.720	41.447 ± 49.777	81.032 ± 70.991	60.412 ± 64.112
pt-reco-4	3.758 ± 0.134	4.028 ± 1.109	261.816 ± 96.423	47.333 ± 52.903	23.149 ± 6.437	15.965 ± 28.100	123.597 ± 65.578	394.563 ± 107.843	34.616 ± 22.830	32.684 ± 48.329	69.403 ± 79.034	51.481 ± 50.419
reco-4	3.637 ± 0.375	3.313 ± 0.643	223.318 ± 88.989	41.457 ± 41.054	17.760 ± 5.380	18.787 ± 40.915	128.605 ± 74.571	372.045 ± 100.057	31.613 ± 21.247	31.097 ± 42.560	55.783 ± 52.321	53.082 ± 52.378
qt-reco-4	3.271 ± 0.406	3.099 ± 0.923	267.139 ± 89.560	51.507 ± 49.455	18.478 ± 5.756	17.875 ± 34.182	135.863 ± 71.914	407.154 ± 86.430	31.978 ± 21.130	26.666 ± 37.319	60.443 ± 58.063	50.702 ± 38.753
qt-reco-4-ns	2.084 ± 0.267	1.156 ± 0.391	220.504 ± 49.952	61.870 ± 66.211	21.708 ± 5.960	13.462 ± 24.528	125.668 ± 50.074	402.748 ± 63.233	29.157 ± 19.563	29.572 ± 35.750	67.997 ± 61.700	44.575 ± 27.637
hardcoded-1	6.486 ± 1.832	26.617 ± 7.624	200.256 ± 65.087	61.268 ± 52.100	11.683 ± 7.774	15.867 ± 27.894	113.038 ± 63.244	394.578 ± 95.579	32.772 ± 26.580	41.489 ± 56.487	81.368 ± 69.214	64.164 ± 72.541
qt-reco-1	2.901 ± 0.609	3.005 ± 1.020	244.099 ± 100.073	49.318 ± 45.511	19.863 ± 8.580	15.005 ± 28.277	127.464 ± 67.042	405.576 ± 66.359	29.161 ± 19.047	27.656 ± 37.383	69.335 ± 70.539	53.770 ± 46.366
qt-reco-6-ns	2.099 ± 0.327	0.893 ± 0.150	224.688 ± 46.879	61.226 ± 61.438	21.702 ± 5.647	14.487 ± 26.782	127.950 ± 54.268	396.338 ± 59.380	29.915 ± 20.218	28.606 ± 35.372	64.242 ± 60.267	50.063 ± 34.534
qt-reco-9-ns	2.199 ± 0.218	2.716 ± 1.116	238.029 ± 86.652	56.751 ± 51.980	21.300 ± 5.790	15.079 ± 27.784	130.979 ± 70.728	407.644 ± 68.638	31.054 ± 20.840	32.416 ± 43.633	76.785 ± 80.134	53.509 ± 44.164
qt-reco-25-ns	1.976 ± 0.173	0.863 ± 0.123	230.240 ± 52.536	58.067 ± 53.512	23.484 ± 5.822	13.652 ± 24.422	123.643 ± 51.230	395.059 ± 64.495	30.882 ± 20.510	29.721 ± 39.078	72.903 ± 74.861	51.196 ± 36.077
qt-outputs-4-ns	2.143 ± 0.417	1.384 ± 0.469	232.550 ± 54.277	60.858 ± 63.674	22.180 ± 6.173	13.206 ± 24.088	127.940 ± 48.767	413.868 ± 70.623	29.645 ± 19.025	29.538 ± 36.087	66.162 ± 59.543	48.303 ± 33.298
qt-covmin-4-ns	2.199 ± 0.220	1.054 ± 0.509	224.056 ± 48.199	61.159 ± 63.017	25.768 ± 5.595	13.498 ± 24.646	126.980 ± 49.664	407.084 ± 70.724	31.167 ± 19.692	32.825 ± 36.941	68.111 ± 63.922	47.500 ± 30.976
qt-covmax-4-ns	2.175 ± 0.214	0.928 ± 0.254	213.556 ± 49.202	59.329 ± 60.668	21.273 ± 5.913	13.184 ± 24.116	125.341 ± 52.401	407.264 ± 66.606	30.564 ± 19.857	30.020 ± 35.265	67.472 ± 63.610	48.234 ± 32.006
qt-cmd-4-ns	2.001 ± 0.233	0.879 ± 0.264	227.694 ± 55.555	63.944 ± 64.977	24.530 ± 7.232	13.675 ± 24.866	130.660 ± 50.915	415.388 ± 67.833	29.847 ± 19.153	30.252 ± 36.339	68.877 ± 64.653	47.890 ± 30.716

Table 4: Mean pairwise KL-coverage of all studied cases over 20 runs and using 10 bins per dimension: reference distributions are computed over the column cases and tested distributions over the row cases (so each pairwise score is averaged over $20 \times 20 = 400$ KL-coverage scores). Lower scores mean distributions that are more similar. The numbers following the symbol \pm represent the standard deviation.